$0\nu\beta\beta$ Matrix Elements with Coupled Cluster Theory

Samuel J. Novario

University of Tennessee
Oak Ridge National Laboratory

September 10, 2019

U.S. DEPARTMENT OF ENERGY

NUCLEI Nuclear Computational Low-Energy Initiative

THE UNIVERSITY OF TENNESSEE KNOXVILLE

OAK RIDGE NATIONAL LABORATORY MANAGED BY UT-BATTELLE FOR THE DEPARTMENT OF ENERGY

Outline

Motivation

$$\left(T_{1/2}^{0\nu}\right)^{-1} = G_{0\nu}\left(Q_{\beta\beta}, Z\right)\left|M^{0\nu}\right|^2\left(\langle m_{\beta\beta}/m_e\rangle\right)^2$$

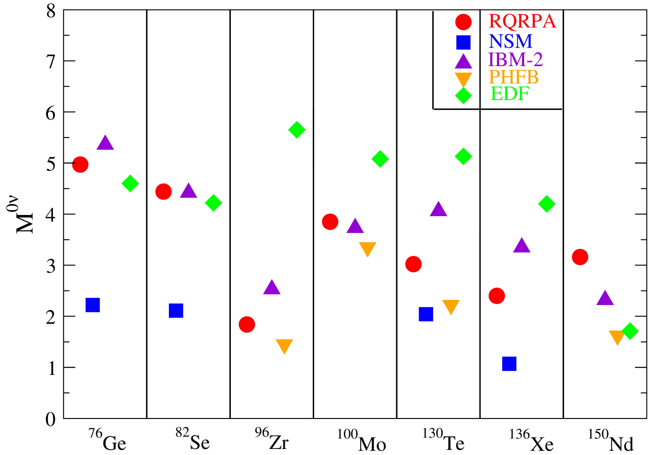

Petr Vogel. 2012. J. Phys. G: Nucl. Part. Phys. 39 124002.

Motivation

$$\left(T^{0\nu}_{1/2}\right)^{-1} = G_{0\nu}\left(Q_{\beta\beta}, Z\right)\left|M^{0\nu}\right|^2\left(\langle m_{\beta\beta}/m_e\rangle\right)^2$$

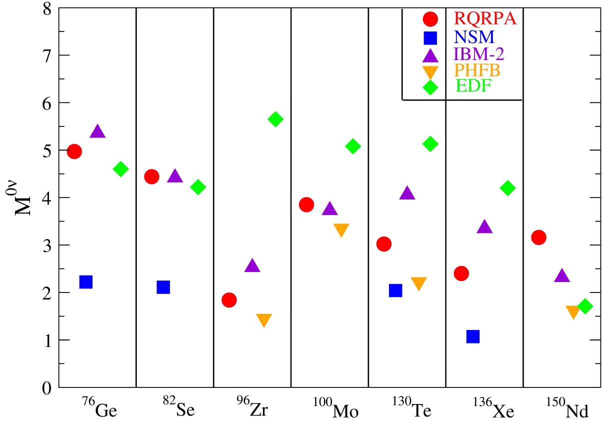

Different models give inconsistent results.

Need precise control of calculation with quantified uncertainties.

Motivates the use of microscopic *ab initio* methods.

Petr Vogel. 2012. J. Phys. G: Nucl. Part. Phys. 39 124002.

Progress of *Ab Initio* Methods

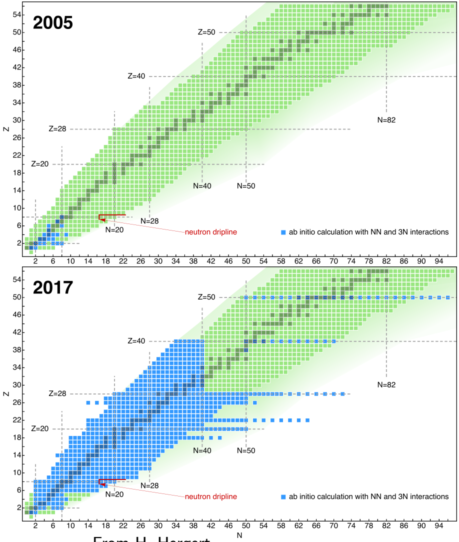

From H. Hergert

Progress of *Ab Initio* Methods

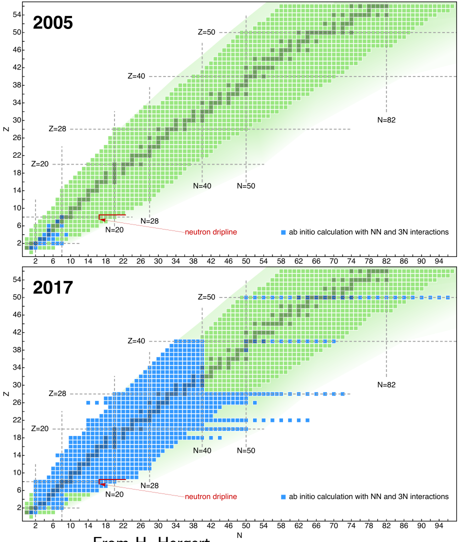

From H. Hergert

Realistic interactions from chiral effective field theory.

RG softening of potentials to reduce correlations.

Exponential improvements in high-performance computing.

Polynomially scaling many-body methods like Coupled Cluster Theory.

Coupled Cluster Theory

Coupled cluster theory is based of the exponential ansatz,

$$|\Psi\rangle = e^{\hat{T}} |\Phi_0\rangle$$

$$\hat{T} \equiv \hat{T}_1 + \hat{T}_2 + \cdots + \hat{T}_A$$

Coupled Cluster Theory

Coupled cluster theory is based of the exponential ansatz,

$$|\Psi\rangle = e^{\hat{T}} |\Phi_0\rangle$$

$$\hat{T} \equiv \hat{T}_1 + \hat{T}_2 + \cdots + \hat{T}_A$$

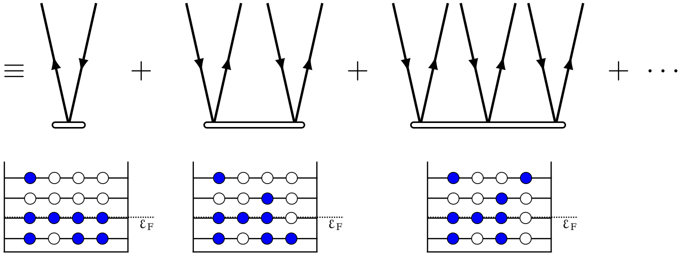

Coupled-Cluster Effective Hamiltonian

- Many-body Schrödinger equation:

$$\hat{H}|\Psi\rangle = \hat{H}\,\mathrm{e}^{\hat{T}}|\Phi_0\rangle = E\,\mathrm{e}^{\hat{T}}|\Phi_0\rangle$$

Coupled-Cluster Effective Hamiltonian

- Many-body Schrödinger equation:

$$\hat{H}|\Psi\rangle = \hat{H}e^{\hat{T}}|\Phi_0\rangle = E\, e^{\hat{T}}|\Phi_0\rangle$$

- Similarity-transformed Hamiltonian:

$$\bar{H} \equiv e^{-\hat{T}}\,\hat{H}e^{\hat{T}}$$

Coupled-Cluster Effective Hamiltonian

- Many-body Schrödinger equation:

$$\hat{H}|\Psi\rangle = \hat{H} e^{\hat{T}} |\Phi_0\rangle = E\, e^{\hat{T}} |\Phi_0\rangle$$

- Similarity-transformed Hamiltonian:

$$\bar{H} \equiv e^{-\hat{T}} \hat{H} e^{\hat{T}}$$

$$\bar{H} = \hat{H} + [\hat{H}, \hat{T}] + \frac{1}{2!}[[\hat{H}, \hat{T}], \hat{T}] + \frac{1}{3!}[[[\hat{H}, \hat{T}], \hat{T}], \hat{T}] + \frac{1}{4!}[[[[\hat{H}, \hat{T}], \hat{T}], \hat{T}], \hat{T}] + \cdots$$

Coupled-Cluster Effective Hamiltonian

- Many-body Schrödinger equation:

$$\hat{H}|\Psi\rangle = \hat{H}e^{\hat{T}}|\Phi_0\rangle = E\,e^{\hat{T}}|\Phi_0\rangle$$

- Similarity-transformed Hamiltonian:

$$\bar{H} \equiv e^{-\hat{T}}\hat{H}e^{\hat{T}}$$

$$\bar{H} = \hat{H} + [\hat{H}, \hat{T}] + \frac{1}{2!}[[\hat{H}, \hat{T}], \hat{T}] + \frac{1}{3!}[[[\hat{H}, \hat{T}], \hat{T}], \hat{T}] + \frac{1}{4!}[[[[\hat{H}, \hat{T}], \hat{T}], \hat{T}], \hat{T}] + \cdots$$

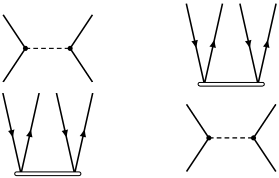

Coupled-Cluster Effective Hamiltonian

- Many-body Schrödinger equation:

$$\hat{H}|\Psi\rangle = \hat{H}e^{\hat{T}}|\Phi_0\rangle = E\,e^{\hat{T}}|\Phi_0\rangle$$

- Similarity-transformed Hamiltonian:

$$\bar{H} \equiv e^{-\hat{T}}\hat{H}e^{\hat{T}}$$

$$\bar{H} = \hat{H} + [\hat{H},\hat{T}] + \frac{1}{2!}[[\hat{H},\hat{T}],\hat{T}] + \frac{1}{3!}[[[\hat{H},\hat{T}],\hat{T}],\hat{T}] + \frac{1}{4!}[[[[\hat{H},\hat{T}],\hat{T}],\hat{T}],\hat{T}] + \cdots$$

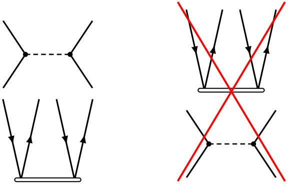

$$\rightarrow \quad \bar{H} = \left(\hat{H}e^{\hat{T}}\right)_c$$

Non-Hermitian Effective Hamiltonian

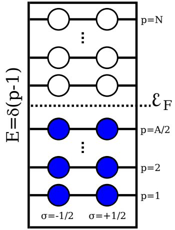

Example: Pairing model at the doubles approximation.

Ground state decoupled from excited states.

All eigenvalues are preserved without truncations and real with an appropriately-conditioned Hamiltonian.

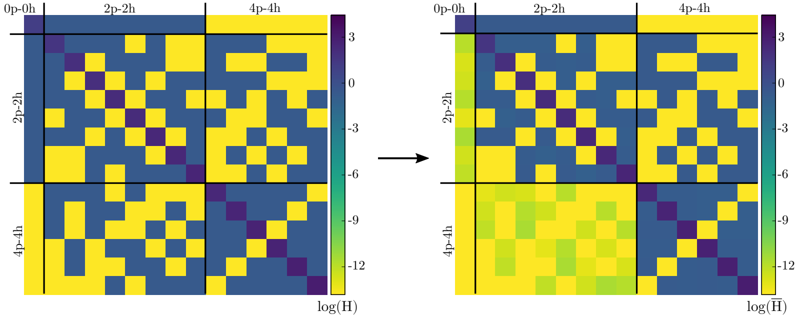

Equation of Motion Method

EOM method builds on the closed-shell ground state,

$$|\Psi_\mu\rangle = \hat{R}_\mu |\Psi\rangle = \hat{R}_\mu \, \mathrm{e}^{\hat{T}} |\Phi_0\rangle$$

$$\hat{R} \equiv r_0 + \hat{R}_1 + \hat{R}_2 + \cdots$$

Equation of Motion Method

EOM method builds on the closed-shell ground state,

$$|\Psi_\mu\rangle = \hat{R}_\mu |\Psi\rangle = \hat{R}_\mu \, e^{\hat{T}} |\Phi_0\rangle$$

$$\hat{R} \equiv r_0 + \hat{R}_1 + \hat{R}_2 + \cdots$$

Double charge exchange EOM

$\hat{R}^{0\nu\beta\beta} \equiv$

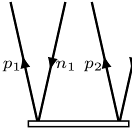

$+$

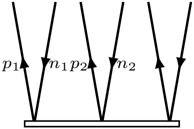

$+ \cdots$

Equation of Motion Method

EOM method builds on the closed-shell ground state,

$$|\Psi_\mu\rangle = \hat{R}_\mu |\Psi\rangle = \hat{R}_\mu \, e^{\hat{T}} |\Phi_0\rangle$$

$$\hat{R} \equiv r_0 + \hat{R}_1 + \hat{R}_2 + \cdots$$

Double charge exchange EOM

$\hat{R}^{0\nu\beta\beta} \equiv$

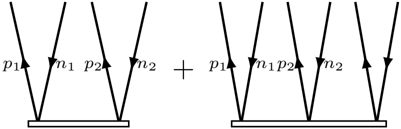

$+ \cdots$

$$\hat{H}\hat{R}_\mu \, e^{\hat{T}} |\Phi_0\rangle = E_\mu \hat{R}_\mu \, e^{\hat{T}} |\Phi_0\rangle$$

$$\left(\bar{H}_{\mathrm{N}} \hat{R}_\mu\right)_c |\Phi_0\rangle = \omega_\mu \hat{R}_\mu |\Phi_0\rangle$$

Dual Solutions

Non-Hermitian $\bar{H}$ has left-eigenvalue problem,

$$\langle\Phi_0|\,\hat{L}_\mu\,\bar{H}_\mathrm{N} = \langle\Phi_0|\,\hat{L}_\mu\omega_\mu,$$

$$\hat{L} \equiv l_0 + \hat{L}_1 + \hat{L}_2 + \cdots$$

Dual Solutions

Non-Hermitian $\bar{H}$ has left-eigenvalue problem,

$$\langle \Phi_0 | \hat{L}_\mu \bar{H}_\mathrm{N} = \langle \Phi_0 | \hat{L}_\mu \omega_\mu,$$

$$\hat{L} \equiv l_0 + \hat{L}_1 + \hat{L}_2 + \cdots$$

Double charge exchange EOM

$\hat{L}^{0\nu\beta\beta} \equiv$ 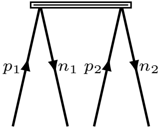 $+$ 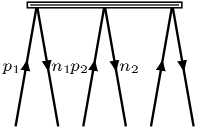 $+ \cdots$

Dual Solutions

Non-Hermitian $\bar{H}$ has left-eigenvalue problem,

$$\langle\Phi_0|\,\hat{L}_\mu\,\bar{H}_{\mathrm{N}} = \langle\Phi_0|\,\hat{L}_\mu\omega_\mu,$$

$$\hat{L} \equiv l_0 + \hat{L}_1 + \hat{L}_2 + \cdots$$

Double charge exchange EOM

$\hat{L}^{0\nu\beta\beta} \equiv$

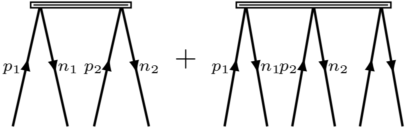

$+ \cdots$

$$\langle\Phi_0|\,\hat{L}_\mu\hat{R}_\nu\,|\Phi_0\rangle = \delta_{\mu\nu}$$

Dual Solutions

Non-Hermitian $\bar{H}$ has left-eigenvalue problem,

$$\langle \Phi_0 | \hat{L}_\mu \bar{H}_\mathrm{N} = \langle \Phi_0 | \hat{L}_\mu \omega_\mu,$$

$$\hat{L} \equiv l_0 + \hat{L}_1 + \hat{L}_2 + \cdots$$

Ground state left eigenvector

$\hat{L}_0 \equiv 1 +$ 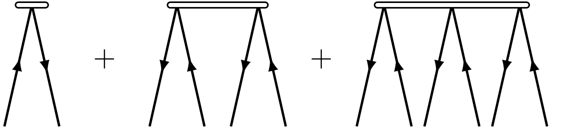 $+ \cdots$

$$\langle \Phi_0 | \hat{L}_0 | \Phi_0 \rangle = 1$$

Coupled Cluster $0\nu\beta\beta$ NME

$0\nu\beta\beta$ operator derived from chiral EFT using the closure approximation

$$\hat{O} = \hat{O}^{0\nu}_{\mathrm{GT}} + \hat{O}^{0\nu}_{\mathrm{F}} + \hat{O}^{0\nu}_{\mathrm{T}}$$

$0\nu\beta\beta$ nuclear matrix element

$$\left|M^{0\nu}\right|^2 = \left|\langle \mathrm{f}|\,\hat{O}\,|\mathrm{i}\rangle\right|^2 = \langle \mathrm{f}|\,\hat{O}\,|\mathrm{i}\rangle\langle \mathrm{i}|\,\hat{O}^\dagger\,|\mathrm{f}\rangle$$

$$= \langle\Phi_0|\,\mathrm{e}^{-\hat{T}}\,\hat{L}_{\mathrm{f}}\hat{O}\,\mathrm{e}^{\hat{T}}\,|\Phi_0\rangle\langle\Phi_0|\,\mathrm{e}^{-\hat{T}}\,\hat{L}_0\,\hat{O}^\dagger\hat{R}_{\mathrm{f}}\,\mathrm{e}^{\hat{T}}\,|\Phi_0\rangle$$

$$= \boxed{\langle\Phi_0|\,\hat{L}_{\mathrm{f}}\,\bar{O}\,|\Phi_0\rangle\langle\Phi_0|\,\hat{L}_0\,\bar{O}^\dagger\hat{R}_{\mathrm{f}}\,|\Phi_0\rangle}$$

Similarity-transformed beta-decay operator

$$\mathrm{e}^{-\hat{T}}\,\hat{O}\,\mathrm{e}^{\hat{T}} = \left(\hat{O}e^{\hat{T}}\right)_{\mathrm{c}}$$

$0\nu\beta\beta$ Benchmarks in Light Nuclei: ^{14}C and ^{10}He

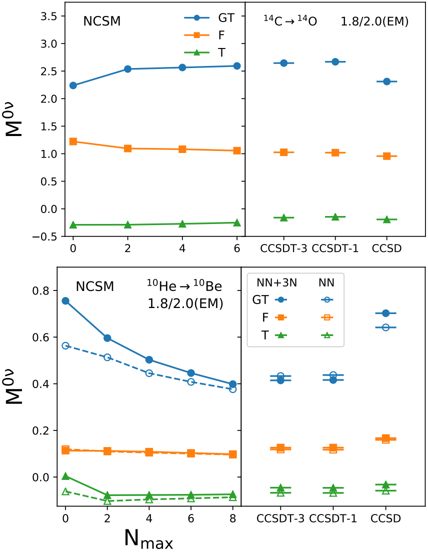

CC calculations of $^{14}\text{C} \rightarrow {}^{14}\text{O}$ agree well with NCSM. The mirror structure of the initial and final nuclei make this comparison somewhat trivial.

CC calculations of $^{10}\text{He} \rightarrow {}^{10}\text{Be}$ also agree with NCSM. The final nuclei has an open-shell structure.

Both of these cases have well-converged initial and final wavefunctions.

$0\nu\beta\beta$ Benchmarks in Light Nuclei: ^{8}He and ^{22}O

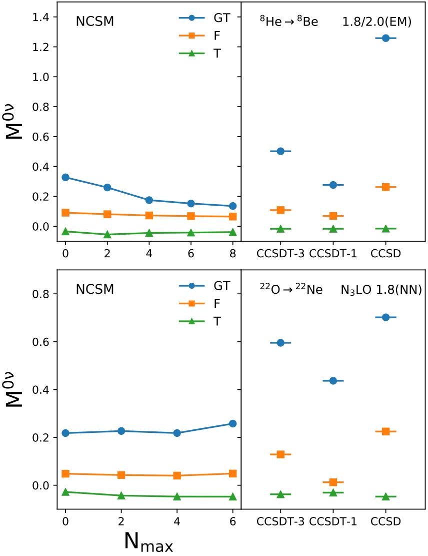

CC calculations of ^{8}He $\rightarrow$ ^{8}Be and ^{22}O $\rightarrow$ ^{22}Ne do not agree well with NCSM.

While the initial wavefunctions are well-converged, the spherical basis does not capture the deformed, open-shell final states.

Describing these states would require correlations beyond double and triple excitations.

$0\nu\beta\beta$ Decay of ^{48}Ca

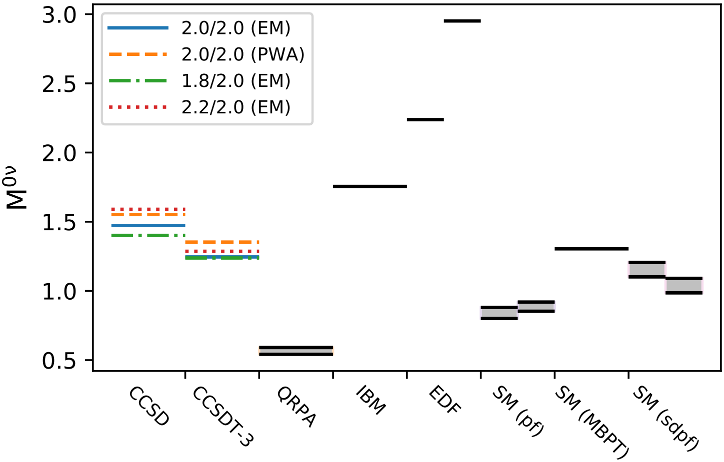

Like the ground states of ^{8}Be and ^{22}Ne, ^{48}Ti has a deformed, open-shell structure.

Spectrum of ^{48}Ti with Spherical Coupled Cluster

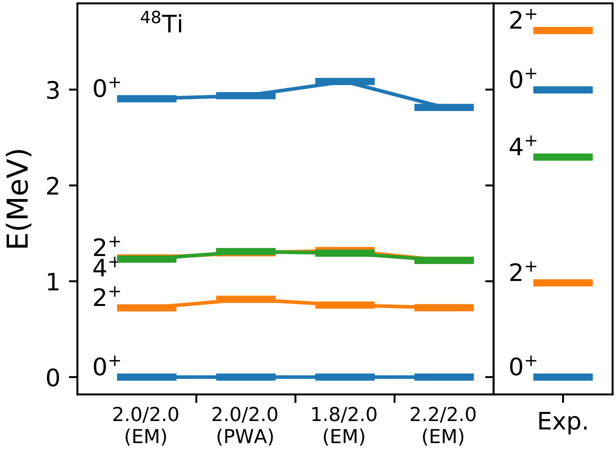

Inability to calculate 4^+ and 2^+ states suggest triples correlations in spherical basis do not capture deformation of ^{48}Ti ground state.

Hartree Fock Basis: Spherical

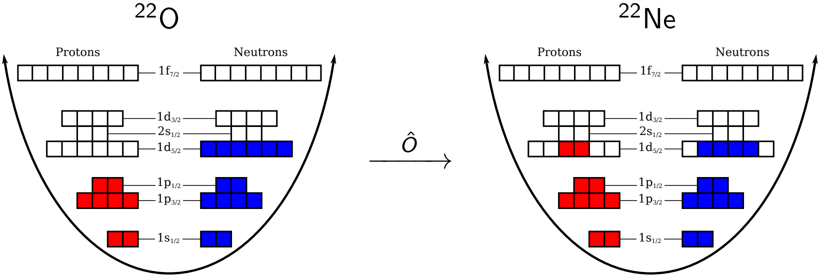

1) Compute spherical HF basis of initial nucleus
2) Decouple initial nucleus ground state
3) Diagonalize EOM ground state of final nucleus

Pros: Maintains total angular momentum and is computationally efficient.

Cons: Cannot feasibly calculate open-shell, deformed nuclei.

Hartree Fock Basis: Deformed

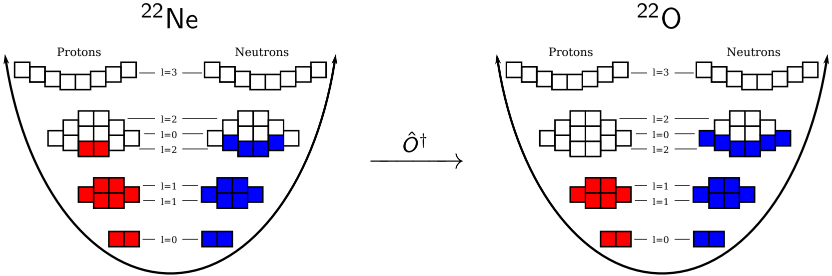

1) Compute deformed HF basis of final nucleus
2) Decouple final nucleus ground state
3) Diagonalize EOM ground state of initial nucleus

Pros: Can calculate open-shell, deformed nuclei without EOM diagonalization.

Cons: Doesn't preserve total angular momentum and is more computationally expensive.

$0\nu\beta\beta$ Benchmarks in Light Nuclei: ^{8}He and ^{22}O

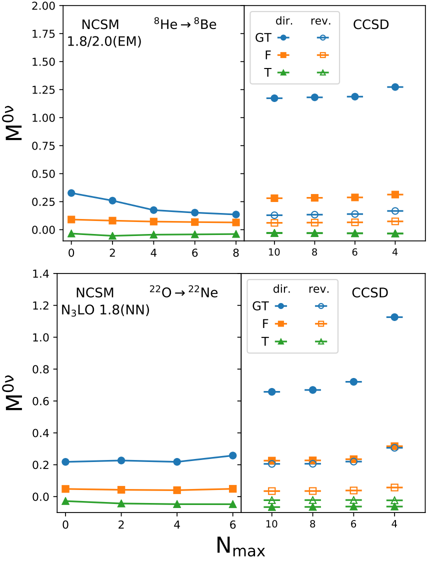

Deformed CC calculations of ^{8}He $\rightarrow$ ^{8}Be and ^{22}O $\rightarrow$ ^{22}Ne agree well with NCSM.

The final deformed nuclei are well described without triples corrections.

The initial spherical nuclei is sufficiently described in the deformed basis.

$0\nu\beta\beta$ Benchmarks in Light Nuclei: ^{14}C and ^{10}He

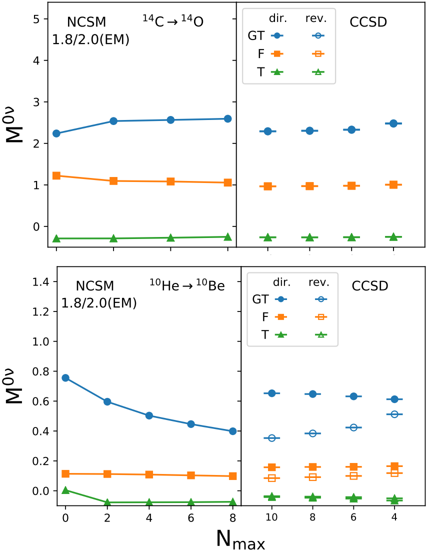

Deformed CC calculations of ^{14}C $\rightarrow$ ^{14}O and ^{10}He $\rightarrow$ ^{10}Be still agree well with NCSM.

Adding triples to the open-shell ^{10}Be can account for the discrpencies between bases and NCSM.

$0\nu\beta\beta$ Decay of ^{48}Ca: Deformed Basis

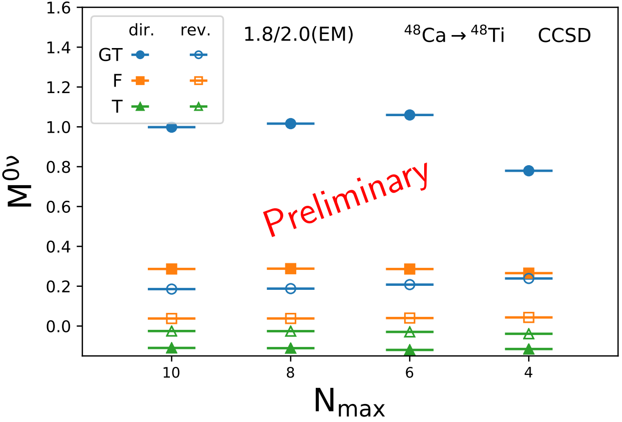

$0\nu\beta\beta$ NME of $^{14}C \rightarrow {}^{14}O$ between $0.20 - 1.17$.

Large difference shows importance of deformation and can be resolved with additional correlations.

Summary

- Coupled cluster $0\nu\beta\beta$ calculations agree well with NCSM benchmarks of light nuclei with well-described final states.
- Deformed coupled cluster can address problems involving open-shell, deformed nuclei.
- The deformed ground state of ^{48}Ti is not easily obtained.
- Both a deformed basis and triples corrections are required to obtain quality ground states for ^{48}Ti and ^{48}Ca.

Current and Future Work

- Add triples correlations and continue convergence studies of ^{48}Ti $\rightarrow$ ^{48}Ca.
- Investigate different deformation parameters of ^{48}Ti.
- Calculate contribution of missing LO contact term.
- Use developed machinery for $2\nu\beta\beta$ decays.
- Use deformed basis to calculate previously intractable case of ^{76}Ge.

Thank You!

- Thomas Papenbrock
- Gaute Hagen
- Gustav Jensen
- Jonathan Engel
- Petr Navratil

U.S. DEPARTMENT OF ENERGY

NUCLEI Nuclear Computational Low-Energy Initiative

THE UNIVERSITY OF TENNESSEE KNOXVILLE

OAK RIDGE NATIONAL LABORATORY
MANAGED BY UT-BATTELLE FOR THE DEPARTMENT OF ENERGY

Coupled Cluster $2\nu\beta\beta$ NME: Continued Fraction Method

$$\left|M^{2\nu}\right|^2 = \left|\sum_\mu \frac{\langle \mathrm{f}|\,\hat{O}\,|1^+_\mu\rangle\langle 1^+_\mu|\,\hat{O}\,|\mathrm{i}\rangle}{E_\mu - E_i + Q_{\beta\beta}/2}\right|^2$$

$$= \langle \mathrm{f}|\,\hat{O}\frac{1}{\hat{H} - E_i + Q_{\beta\beta}/2}\hat{O}\,|\mathrm{i}\rangle\langle \mathrm{i}|\,\hat{O}^\dagger\frac{1}{\hat{H} - E_i + Q_{\beta\beta}/2}\hat{O}^\dagger\,|\mathrm{f}\rangle$$

$$= \langle \Phi_0|\,\hat{L}_\mathrm{f}\,\bar{O}\frac{1}{\bar{H} - E_i + Q_{\beta\beta}/2}\bar{O}\,|\Phi_0\rangle\langle \Phi_0|\,\hat{L}_0\,\bar{O}^\dagger\frac{1}{\bar{H} - E_i + Q_{\beta\beta}/2}\bar{O}^\dagger\,\hat{R}_\mathrm{f}\,|\Phi_0\rangle$$

Coupled Cluster $2\nu\beta\beta$ NME: Continued Fraction Method

$$\left|M^{2\nu}\right|^2 = \langle\Phi_0|\,\hat{L}_\mathrm{f}\,\bar{O}\,\frac{1}{\bar{H} - E_i + Q_{\beta\beta}/2}\,\bar{O}\,|\Phi_0\rangle\langle\Phi_0|\,\hat{L}_0\,\bar{O}^\dagger\,\frac{1}{\bar{H} - E_i + Q_{\beta\beta}/2}\,\bar{O}^\dagger\,\hat{R}_\mathrm{f}\,|\Phi_0\rangle$$

Define left/right Lanczos pivot vectors for initial and final nuclei

$$\langle\tilde{\nu}_\mathrm{f}| = \langle\Phi_0|\,\hat{L}_\mathrm{f}\,\bar{O} \quad |\nu_\mathrm{i}\rangle = \bar{O}\,|\Phi_0\rangle \quad \langle\tilde{\nu}_\mathrm{i}| = \langle\Phi_0|\,\hat{L}_0\,\bar{O}^\dagger \quad |\nu_\mathrm{f}\rangle = \bar{O}^\dagger\,\hat{R}_\mathrm{f}\langle\Phi_0|$$

Use left/right Lanczos coefficients for continued fraction

$$\left|M^{2\nu}\right|^2 = \langle\tilde{\nu}_\mathrm{f}|\nu_\mathrm{i}\rangle \left[\frac{1}{a_0 - Q_{\beta\beta} - \frac{b_0^2}{a_1 - Q_{\beta\beta} - \frac{b_1^2}{\cdots}}}\right] \langle\tilde{\nu}_\mathrm{i}|\nu_\mathrm{f}\rangle \left[\frac{1}{a_0^\dagger - Q_{\beta\beta} - \frac{b_0^{\dagger 2}}{a_1^\dagger - Q_{\beta\beta} - \frac{b_1^{\dagger 2}}{\cdots}}}\right]$$

Converges to machine precision after $\sim$10 iterations.

Summing explicitly takes $\sim$50 intermediate states with 300-400 iterations.

$2\nu\beta\beta$ Decay Benchmark

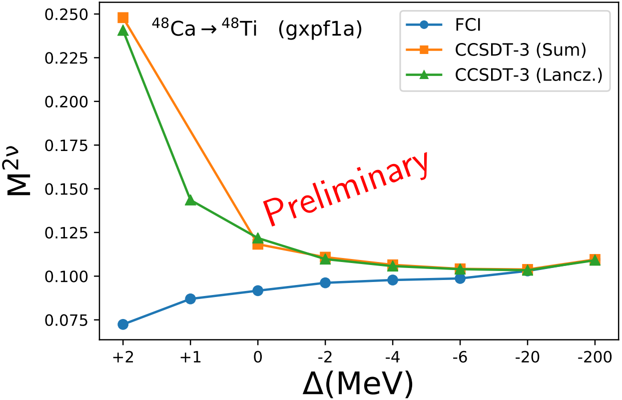

$2\nu\beta\beta$ calculations with phenomenological interaction converge with FCI at large Fermi gap.

The Lanczos continued fraction method also agrees with summing over intermediate ^{48}Sc 1^+ states.

$2\nu\beta\beta$ of ^{48}Ca

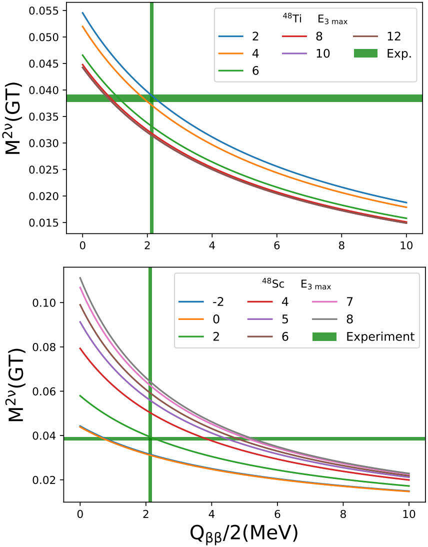

Spherical CC calculations do not reproduce the $Q_{\beta\beta}$-value in this case, so the experimental value is used.

The $2\nu\beta\beta$ calculations converge for sufficient $E_{3\ max}(^{48}\text{Ti})$ and $E_{3\ max}(^{48}\text{Ca})$.

Given the results for $0\nu\beta\beta$ and the deformation of ^{48}Ti, a deformed basis with triples is probably necessary.